THE NATURE OF INVISIBLE GOLD IN SULFIDES FROM THE XIANGXI Au–Sb–W ORE DEPOSIT IN NORTHWESTERN HUNAN, PEOPLE'S REPUBLIC OF CHINA

SIXUE YANG[1]

Freie Universität Berlin, FR Rohstoff- und Umweltgeologie, Malteserstrasse 74-100, D-12249 Berlin, Germany

NORBERT BLUM[2]

Forschungszentrum Jülich, Projektträger BEO, Seestrasse 15, D-18119 Warnemünde, Germany

ERIO RAHDERS

Freie Universität Berlin, FR Rohstoff- und Umweltgeologie, Malteserstrasse 74-100, D-12249 Berlin, Germany

ZHENRU ZHANG

Department of Geology, Central-South University of Technology, Changsha 410083, People's Republic of China

ABSTRACT

Pyrite from the red-slate-hosted Proterozoic Xiangxi Au–Sb–W deposit in northwestern Hunan Province, China, was studied to determine the nature of the invisible gold that it contains. TEM measurements, confirmed by EDS, reveal that some of the submicrometer gold occurs mainly as 0.07–0.15 µm spheres on growth surfaces of the pyrite and in microfissures in stibnite. Application of the Lamb–Mössbauer effect to results of analyses by ^{197}Au Mössbauer spectroscopy indicates that 89% of the gold in pyrite crystals occurs in the metallic state, and that 11% is chemically bound. Considerations of crystal chemistry and updated experimental and analytical data on As–Sb sulfide systems, particularly pyrite – arsenopyrite – löllingite, indicate that chemically bound gold may occur in octahedra, comprised most likely of $AuAs_2$, likely of $AuAsS$, or less likely of AuS_2, in As-bearing pyrite and arsenopyrite. The valence, structure, and coordination of chemically bound gold in the octahedra are probably intermediate between those in pyrite and in aurostibite.

Keywords: invisible gold, Au-bearing octahedra, sulfides, transmission electron microscopy, ^{197}Au Mössbauer spectroscopy, Xiangxi, People's Republic of China.

SOMMAIRE

Nous avons étudié la pyrite dans les ardoises rouges protérozoïques du gisement à Au–Sb–W de Xiangsi, situé dans le nord–ouest de la province de Hunan, en Chine, afin de déterminer la nature de l'or invisible qu'elle contient. Les mesures, effectuées par microscopie électronique par transmission et confirmées par analyses en dispersion d'énergie, révèlent qu'une partie de l'or submicrométrique s'y présente surtout sous forme de sphérules de 0.07–0.15 µm sur les surfaces de croissance de la pyrite et dans les microfissures de la stibnite. L'application de l'effet Lamb–Mössbauer aux résultats des analyses par spectroscopie ^{197}Au de Mössbauer montre que 89% de l'or dans les cristaux de pyrite se trouvent à l'état métallique, et que 11% s'y trouve sous une forme liée chimiquement. Des considérations de chimie cristalline et des données expérimentales et analytiques récentes sur les systèmes de sulfures As–Sb, particulièrement pyrite – arsénopyrite – löllingite, indiquent que l'or lié chimiquement serait présent en coordinence octaédrique; il est très probable que les agencements impliquent $AuAs_2$, probable qu'ils impliquent $AuAsS$, et moins probable qu'il y ait des agencements AuS_2 dans la pyrite contenant l'arsenic ou dans l'arsénopyrite. La valence, structure, et coordinence de l'or lié chimiquement en octaèdres seraient intermédiaires entre celles de la pyrite et celles de l'aurostibite.

(Traduit par la Rédaction)

Mots-clés: or invisible, octaèdres aurifères, sulfures, microscopie électronique par transmission, spectroscopie ^{197}Au de Mössbauer, Xiangxi, République Populaire de Chine.

---

[1] Corresponding author. *E-mail address*: cbysx@zedat.fu-berlin.de
[2] *E-mail address*: n.blum@fz-juelich.de

INTRODUCTION

The existence of invisible gold, *i.e.*, gold not detectable under the ore microscope, has long been noted by many investigators (*e.g.*, Stillwell & Edwards 1946, Joralemon 1951, Boyle 1979, Cabri 1988, Cabri *et al.* 1989). Because of its very small size, such invisible gold is not only difficult to identify, but also hard to recover from ore materials (refractory Au). At the same time, there is a poor understanding of the nature of its occurrence in sulfides.

Fleet & Mumin (1997) and Cook & Chryssoulis (1990) reviewed different analytical methods to search for invisible gold. Farges *et al.* (1993) worked on the local environment around Au^{3+} in aqueous chloride solutions, employing the extended X-ray absorption fine structure (EXAFS) technique; however, its use for studying natural gold-bearing minerals remains insufficiently tested. Li *et al.* (1995) studied chemically bound gold in sulfides from Carlin-type deposits and in synthetic samples with X-ray photoelectron spectroscopy (XPS). With this technique, Jean & Bancroft (1985), Bancroft & Hyland (1990), and Mycroft *et al.* (1995) investigated the processes of deposition and reduction of gold on the surfaces of sulfides from solutions containing gold ions and chloride. Becker *et al.* (1997) also investigated these mechanisms on galena surfaces with XPS and scanning tunneling spectroscopy (STS). These investigations indicate that the reduction of gold (Au^0) on the surface of sulfides from $AuCl_4$-bearing solutions proceeds rapidly. Theoretically, a field ion microscope (FIM) also can be used to analyze chemically bound gold in sulfides, but there is as yet no report of a successful application. Secondary ion mass spectroscopy (SIMS) is a far more sensitive analytical technique frequently applied, which provides ion imaging and depth profiles (*e.g.*, Cook & Chryssoulis 1990).

Here, we classify the techniques used for detection of gold as methods of direct observation, analytical methods, and combined methods. Methods of direct observation allow the determination of the morphology of gold and its location in host minerals (high-resolution transmission electron microscopy [TEM]). With some spectroscopic analytical methods, gold can be identified or its concentration quantified in its host minerals ([197]Au Mössbauer spectroscopy and X-ray photoelectron spectroscopy [XPS]). A combination of methods of observation and analytical techniques allows one to study the morphology of gold and chemical components (TEM with energy-dispersion X-ray spectrometry [EDS], FIM, and SIMS). Studies of invisible gold are aimed at the identification of gold and a detection of its location at surfaces and along fissures on or in host minerals. Depending on its state, invisible gold can be divided into submicrometer-size gold and chemically bound gold (Table 1).

Cathelineau *et al.* (1988) suggested that an Au^{3+}-bearing phase of unknown stoichiometry may

TABLE 1. CLASSIFICATION OF GOLD PARTICLES ACCORDING TO TO THEIR SIZE, XIANXI Au DEPOSIT, PEOPLE'S REPUBLIC OF CHINA

Types	Visible Gold		Invisible Gold	
Subtype	Macroscopic particles of gold	Micrometric particles of gold	Submicrometric particles of gold	Chemically bound gold
Size range	>100 µm	≤100 to 1 µm	<1 µm to ≥2.8 Å	<2.8 Å
Methods of detection	eye, binocular, magnifying glass	optical microscopy, magnifying glass, SEM, EDS, WDS	TEM with EDS, high-resolution TEM, XPS, SIMS, [197]Au Mössbauer	SIMS, [197]Au, Mössbauer, XPS, FIM

Practical maximum resolution of microscopy is 1 µm (theoretical resolution: 0.26 µm). EDS: energy-dispersion X-ray spectrometry; FIM: field ion microscopy. Mössbauer: Mössbauer spectroscopy; SEM: scanning electron microscopy; SIMS: secondary ion mass spectroscopy; TEM: transmission electron microscopy; WDS: wavelength-dispersion X-ray spectrometry; XPS: X-ray photoelectron spectroscopy. 10^{-3} mm = 1 µm = 10^4 Å.

exist, such as (Fe,Au,As). Arehart *et al.* (1993) postulated a substitution of Au^{3+} for Fe^{2+} in arsenopyrite. Friedl (1993) has measured spectra of chemically bound gold in pyrite and arsenopyrite, but did not resolve the question of the state of bonding and valence of gold in the sulfides. Fleet *et al.* (1993) concluded that gold is probably incorporated into a metastable solid-solution in arsenian pyrite *via* As-rich growth surfaces. Mumin *et al.* (1994) suggested that most of the primary gold precipitated as a solid solution, and was redistributed to form colloidal and micrometer-size particles of gold following various changes of state. Li *et al.* (1995) reported that gold may exist as negative ions in sulfides from Carlin-type deposits and in synthetic sulfide samples. Fleet & Mumin (1997) suggested that invisible gold in arsenian pyrite, marcasite and arsenopyrite from Carlin Trend gold deposits and synthesized in the laboratory was removed from ore fluids by chemisorption at As-rich, Fe-deficient surface sites, and incorporated into the solids in metastable solid-solution. However, the oxidation state of invisible gold, particularly chemically bound gold, remains uncertain because the chemisorption process is intrinsically non-systematic in terms of crystal-chemical parameters, and does not result in definitive atomic substitution trends. There is as yet no satisfactory explanation about the nature of the invisible, particularly chemically bound gold in sulfides, mainly in pyrite and arsenopyrite.

In this paper, we examine submicrometer-size particles of gold in sulfides, arsenian pyrite and stibnite from the Xiangxi Au–Sb–W mesothermal to epithermal ore deposit in northwestern Hunan, China, with the help of combined TEM and EDS. In the mine, macroscopic and micrometer-size gold is scarce, particularly in pyrite with high gold contents. Therefore, the question to be answered is how the gold occurs in pyrite, as chemically bound gold or as submicrometer-size gold or both,
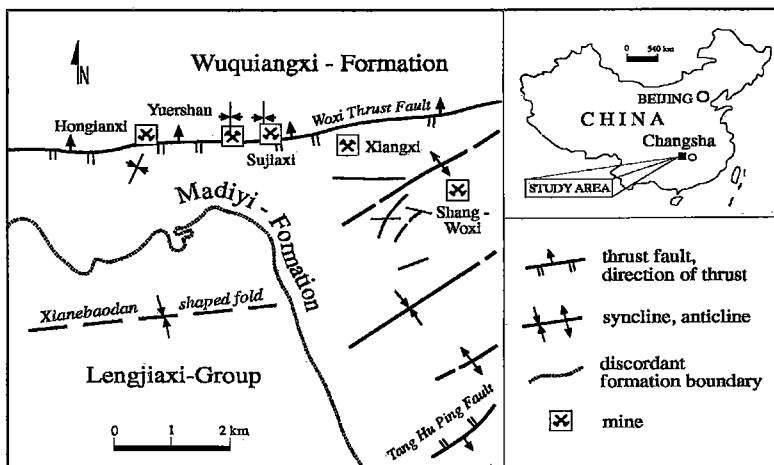
FIG. 1. Simplified geological map of the Xiangxi Au–Sb–W ore deposit in northwestern Hunan, People's Republic of China.

and in which quantities? Metallic and chemically bound gold in concentrates of arsenian pyrite were studied by [197]Au Mössbauer spectroscopy, allowing determination of the various states of gold. On the basis of crystal-chemical data, the possible nature of chemically bound gold in arsenian pyrite and arsenopyrite is constrained.

GEOLOGY AND MINERALOGY AT XIANGXI

The Xiangxi Au–Sb–W deposit is located in northwestern Hunan Province, southeastern China. Late Proterozoic low-grade metamorphic rocks dominate in this area (Fig. 1); the stratigraphic sequence is comprised of: (1) the Lengjiaxi Group (base) with sandy, greyish green slates and locally phyllites, and (2) the Banxi Group (top), comprised of (a) the Madiyi Formation of red slates, locally interbedded with sandy rocks and sandstones, and (b) the Wuqiangxi Formation of sandy, greyish green slates, arkoses and sandstones. The Madiyi Formation is a very important host unit for gold deposits in northwestern Hunan.

Deposits previously exploited in the Xiangxi mining district are Hongianxi, Yuershan, Sujiaxi and Shang-Woxi. Xiangxi is the largest one, and is still being mined (Fig. 1). The mineralization is controlled by the E–W-striking Woxi thrust fault and by anticlines and synclines. At the fault, the Madiyi Formation dips under the younger Wuqiangxi Formation. To the southwest, the Lengjiaxi Group is disconformably overlain by the Madiyi Formation.

The deposit occurs as a mesothermal to epithermal stratabound orebody in red slates of the Madiyi Formation. The mineralization may be associated with a magmatic intrusion (Yang 1995). According to optical examination by ore microscopy and field observations,

the paragenesis of the mineralization can be grouped into four stages (Table 2): (1) scheelite – quartz, (2) pyrite – gold – quartz with minor amounts of arsenopyrite, (3) stibnite – gold – quartz with subordinate amounts of galena and sphalerite, and (4) calcite – quartz. The first and last stage are barren of noble-metal mineralization. Gold in the deposit was mainly deposited in the second and, to a lesser extent, in the third stage of mineralization (Table 2).

Pyrite is the major gold-bearing mineral of the second stage. Two types were identified in microscopic studies. Fine-grained (0.02–0.10 mm) pyrite (I), occurring in significant amounts in ore veins, is commonly anhedral, but occasionally also euhedral (cubes). Coarse-grained pyrite (II) is found in larger quantities in alteration haloes of the host rock. These aggregates

TABLE 2. MINERAL PARAGENESES OF THE XIANGXI DEPOSIT, PEOPLE'S REPUBLIC OF CHINA

Minerals	Stages of Mineralization			
	Scheelite-Quartz	Pyrite-Gold-Quartz	Gold-Stibnite-Quartz	Calcite-Quartz
Sericite	———			———
Scheelite	———			
Wolframite	———			
Quartz	———	———	———	———
Pyrite in host rocks	———			
Pyrite in ore veins		———	———	
Gold		———	———	
Arsenopyrite*		———	———	
Cinnabar			———	
Galena			———	
Sphalerite			———	
Bournonite			———	
Chalcopyrite			———	
Stannite*			———	
Stibnite*			———	
Calcite			———	———
Chlorite				———

* According to Xiangxi mine information

of sulfides range between 1 and 5 mm in size, and are usually euhedral. Their gold concentration is much lower than that of the fine-grained pyrite.

Stibnite of the third stage occurs mainly in ore veins as massive aggregates, measuring 0.01–0.30 mm across. Subordinate amounts of galena and sphalerite with traces of bournonite, chalcopyrite, cinnabar, and stannite were found only in isolated spots within the deposit (Table 2).

According to available information at the Xiangxi mine and our optical studies, micrometer-size gold of the second and third stage occurs mainly in quartz (68% of all gold exploited), in fine-grained pyrite (21%), to a lesser extent in stibnite (<6%) and scheelite (<5%), and in subordinate quantities in other minerals.

The fineness [Au*1000/(Au + Ag)] of native gold at Xiangxi (and also in all other gold deposits of this type in northwestern Hunan), studied by wavelength-dispersion spectrometry (WDS), is very high (Yang 1995). Except for gold inclusions in galena and sphalerite (fineness: 964), Au in quartz, pyrite, stibnite, and scheelite is almost pure (fineness up to 1000). The reason for the extremely high fineness of gold in the Xiangxi mining district and at the Xiangxi mine may be the high content

of reduced sulfur and the very low concentration of Cl (Henley 1985, Niu & Ma 1991). At Xiangxi, the concentration of gold (determined with an Emission Spectrometer [EDS] after preconcentration at the Geoanalytical Center in Hubei, China) in the ore veins and in altered rocks correlates well with sulfur contents (quantified with LECO technology in Hubei), but not as well with arsenic content (measured with an atomic fluorescence spectrometer [AFS] in Hubei) (Fig. 2).

Arsenopyrite commonly contains higher concentrations of gold than pyrite. However, microscopic observations of 30 pyrite – gold – quartz and stibnite – gold – quartz polished ore sections did not reveal any arsenopyrite. According to available information at the Xiangxi mine, this sulfide mineral occurs in very minute amounts in the second stage of mineralization (Table 2). Contents of arsenic in a quartz-bearing pyrite of this fine-grained type are 0.44 wt.% (determination by instrumental neutron-activation analysis, INAA). A back-scattered electron image of arsenic in the mineral concentrate from such pyrite specimens shows As-rich growth bands (with concentrations in the 0.7–2.2 mole % range) in fine-grained pyrite (Fig. 3), suggesting changing physicochemical conditions in ore-forming fluids.
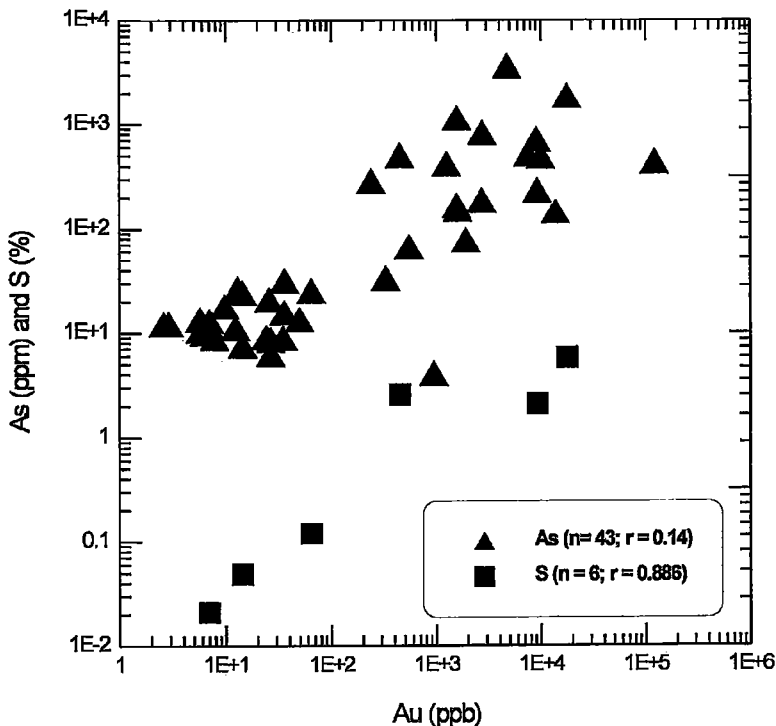

FIG. 2. Concentration of Au *versus* that of As and S in ore veins and in altered host-rocks of the Xiangxi deposit (a log–log diagram is used here because the contents of the selected elements cover a large range). n: numbers of samples, r: correlation coefficient.
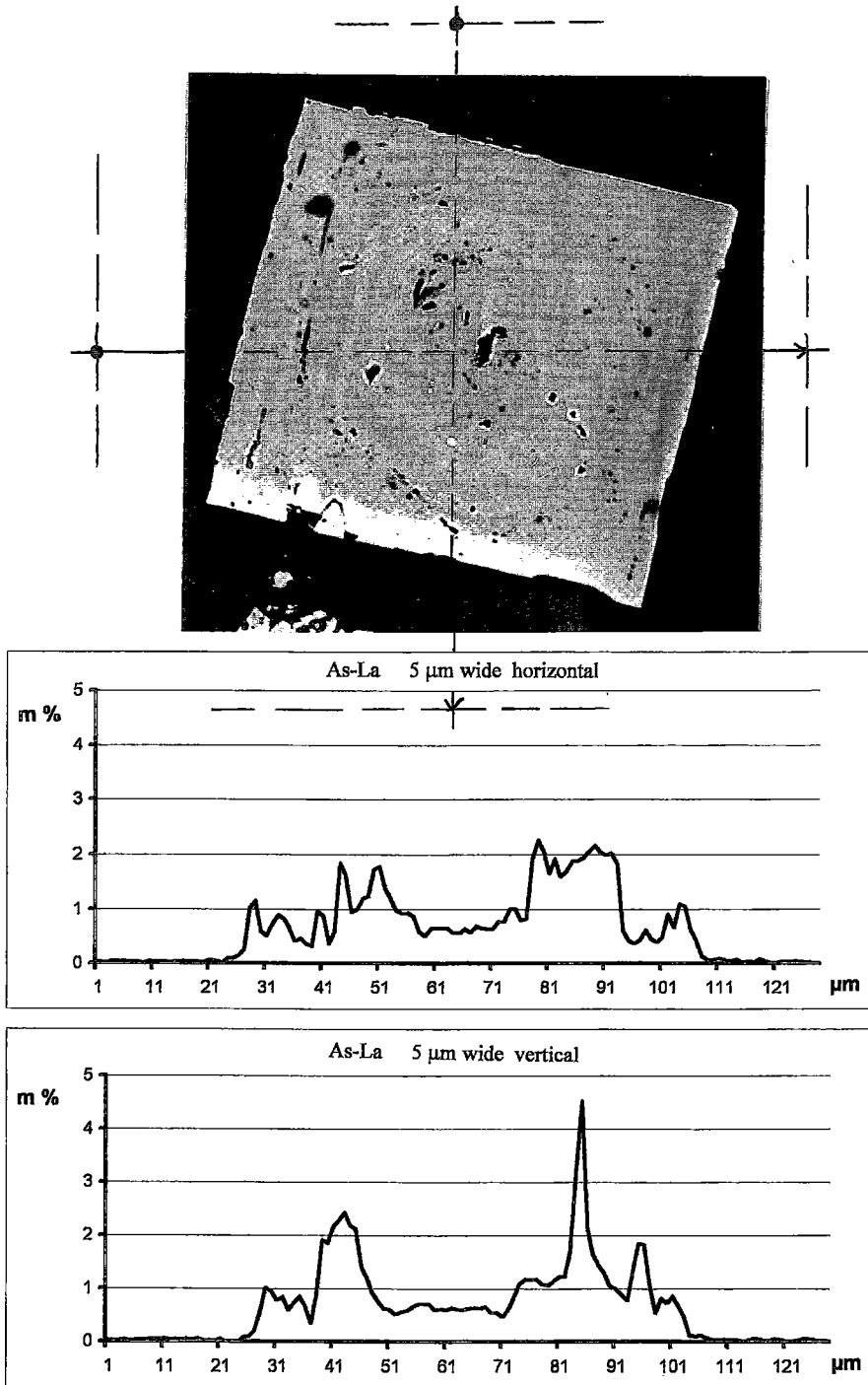
FIG. 3. Back-scattered electron image of arsenic in a crystal of fine-grained pyrite from the Xiangxi deposit, showing As-rich growth bands (with an As content in the range 0.7 to 2.2 mole %). A light circle in the perpendicular line of this picture may result from the small grain of arsenopyrite in the pyrite (analyzed at the Bundesanstalt für Materialforschung und Materialprüfung, Berlin, with a JEOL 733 electron microprobe; analytical conditions: 18 kV, 50 nA; standard: CoAsS for arsenic).

Host rocks in the immediate vicinity of the vein-type mineralization (up to 0.5 m distance) are strongly altered in both footwall and hanging-wall portions. Five major types of alteration are recognized: pyritization, silification, carbonatization, chloritization, and sericitization. Pyritization serves as a very important indicator of gold mineralization in the Xiangxi mining district.

ANALYTICAL METHODS AND SAMPLE DESCRIPTION

Transmission electron microscopy

Specimens for TEM measurements were taken from ore-vein locations with high concentrations of Au in the Xiangxi mine. Studies of submicrometer-size gold in sulfides were carried out with a H–800 TEM, combined with EDS, at the Department of Materials Science of the Central South University of Technology, Changsha, China. The analytical conditions were: accelerating voltage 100 kV, beam current 10 μA. The preparation of the samples for the TEM measurement is based on the "covering – extracting" method, outlined by Zhang et al. (1991). The gold samples prepared by this method contain in principle only undissolved submicrometer-size mineral phases, such as native gold, but no other dissolvable minerals or elements such as As; the sulfides were dissolved.

^{197}Au Mössbauer spectroscopy

Specimens for ^{197}Au Mössbauer measurements originate from the same location as the pyrite samples studied by TEM. Pyrite concentrates were separated using a gravity table. These mineral concentrates contain also quartz (5%) and scheelite (~3%). Arsenopyrite, which commonly shows higher concentrations of gold than pyrite, is scarce at Xiangxi, and was not observed in the pyrite concentrates. Analysis of these sulfide concentrates by GFAAS (Graphite Furnace atomic absorption spectroscopy) yielded an average concentration of 451 ppm Au. Except for very few grains of aurostibite ($AuSb_2$), no other gold mineral was found at Xiangxi (Chen et al. 1991).

For ^{197}Au Mössbauer measurements, we prepared four specimens of the highly gold-enriched material: a coarse gold – quartz sample, a pyrite concentrate, and two specimens of roasted pyrite from the pyrite concentrate. All ^{197}Au Mössbauer measurements were carried out at the Department of Physics at Munich Technical University, Germany. The experimental setup was described by Wagner et al. (1988, 1994).

RESULTS: SUBMICROMETER-SIZE GOLD STUDIED WITH COUPLED TEM–EDS

Pyrite

TEM studies of pyrite reveal that submicrometer-size gold occurs as chains on the growth surfaces (Fig. 4a)

or as individual spheres, ranging mainly from 0.1 to 0.2 μm (averaging 0.15 μm) on the surfaces of pyrite (Fig. 4b). EDS analyses of the spheres show a peak of $AuL\alpha_1$ at 9.713 keV, confirming that these accumulations consist indeed of gold. The distribution of gold on inner growth-surfaces of pyrite is evidence that the submicrometer-size gold coprecipitated with the pyrite.

Stibnite

TEM studies of stibnite indicate that submicrometer-size gold forms spheres measuring 0.04–0.10 μm (average: 0.07 μm), located in micrometric fissures or in grain interstices of stibnite (Fig. 4c). EDS analyses prove that these spheres also consist of gold.

RESULTS: STUDIES OF GOLD IN PYRITE CONCENTRATES BY ^{197}Au MÖSSBAUER SPECTROSCOPY

Metallic gold

The ^{197}Au Mössbauer spectrum of a specimen of coarse gold, sampled from a quartz vein together with fine-grained aggregates of pyrite, yields a single peak of transmission with an isomer shift (IS) value of –1.24 ± 0.001 mm/s (Fig. 5a). This is similar to the IS value of the larger of the two peaks (–1.30 ± 0.02 mm/s) yielded by gold in pyrite concentrates from the Xiangxi deposit (Fig. 5b). This peak can only result from metallic gold, although its IS value is more negative than that of metallic Au in standard sample material (–1.22 ± 0.01 mm/s; Friedl et al. 1992). That the IS value of gold with a high fineness is more strongly negative than that of standard gold, was also described by Wagner et al. (1986, 1988, 1989), and may be typical for Au with high fineness in natural Fe-bearing minerals.

In addition, we roasted part of the pyrite concentrate at temperatures of 450°C and 850°C. The sample roasted at 450°C yields two peaks (Fig. 5c); the larger peak has an IS value of –1.27 ± 0.02 mm/s, similar to the IS value of the large peak in the pyrite concentrate (Fig. 5b). The large peak in the pyrite concentrate roasted at 450°C is comparatively larger than that in the original FeS_2 concentrate; the small one, in contrast, is smaller than that in the original pyrite concentrate. FeS_2 roasted at 850°C shows only one peak, with IS = –1.28 ± 0.02 mm/s (Fig. 5d). The other peak disappeared as a result of high-temperature roasting, pointing to the destruction of the pyrite structure, as was previously suggested by Wagner et al. (1986, 1988).

Chemically bound gold

The smaller peaks in Figures 5b (+3.31 ± 0.24 mm/s) and 5c (+3.29 ± 0.25 mm/s) may result from chemically bound gold in the pyrite concentrate. These peaks cannot be explained by the spectra of known gold minerals (Wagner et al. 1988, 1994), such as aurostibite (IS = +2.33 mm/s) and criddleite (IS = +2.36 mm/s)
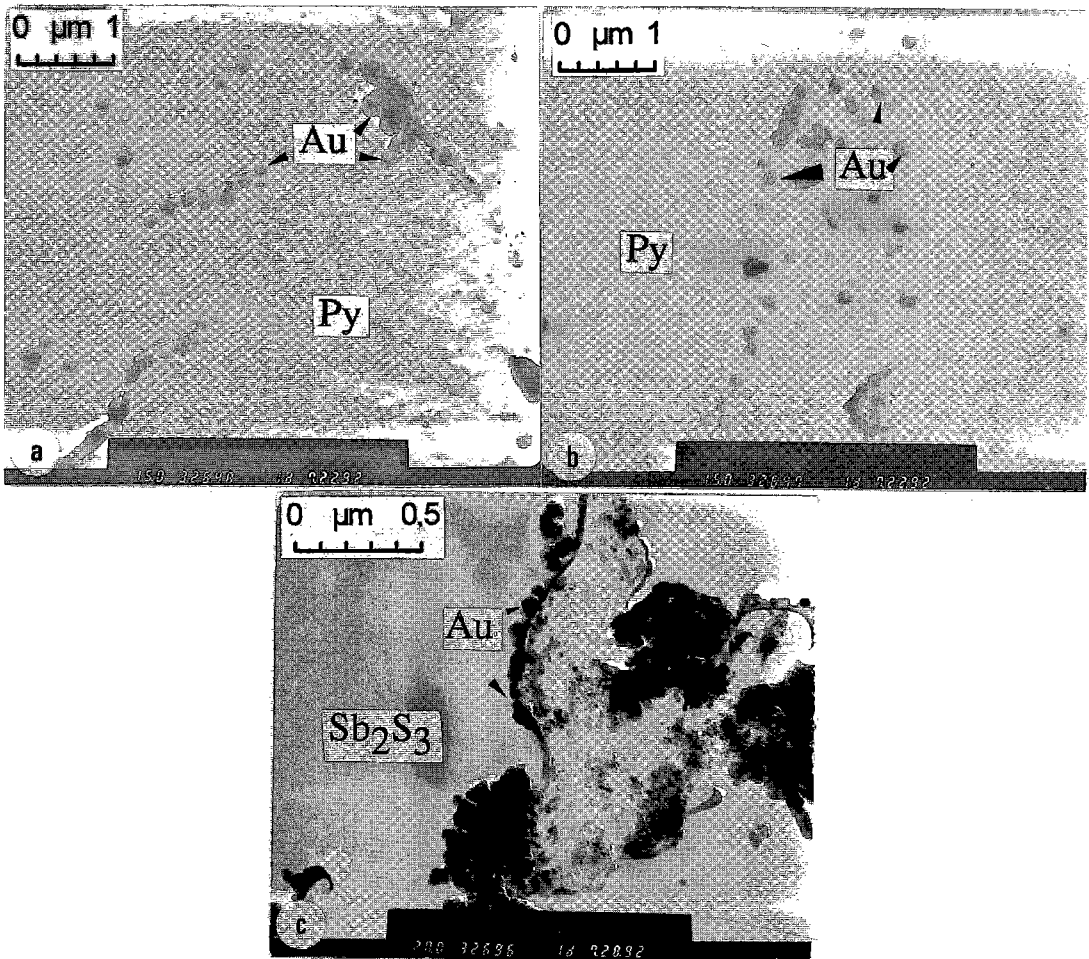
FIG. 4. TEM (transmission electron microscopy) photomicrographs of submicrometer-size gold in sulfides from the Xiangxi deposit: (a) submicrometric gold (size: 0.10–0.20 μm) on the inner growth surface of pyrite; (b) submicrometric gold (size: 0.10–0.22 μm) on the surface of a pyrite sample; (c) submicrometric gold (size: 0.04–0.10 μm) in micrometric fissures or between interstices of stibnite grains.

(Friedl *et al.* 1992). The IS values for chemically bound gold in sulfides fall into the +2.5 – +4.0 mm/s range [*e.g.*, pyrite: +2.5 – +4.0 mm/s, arsenopyrite: +3.0 – +3.8 mm/s; Friedl (1993)]. Compared to the original sulfide concentrate, the size of this small peak decreases in the roasted pyrite at 450°C, and completely disappears in the roasted FeS$_2$ concentrate at 850°C with the destruction of the pyrite structure. This small peak could result from chemically bound gold in the pyrite concentrate.

The content of chemically bound gold in the FeS$_2$ concentrate can be calculated. A ^{197}Au Mössbauer study of the same amount of metallic gold and chemically bound gold at identical conditions, with an identical thickness (d) of specimens, shows that the Lamb –

Mössbauer effect (f) of metallic gold and chemically bound gold (f$_{ch.Au}$/f$_{met.Au}$) (Friedl *et al.* 1992, Friedl 1993) is:

$$A_{ch.Au}/A_{met.Au} = (d_{ch.Au}/d_{met.Au})*(f_{ch.Au}/f_{met.Au}) = (f_{ch.Au}/f_{met.Au}) = 1.625.$$

Here, A represents the area of the peaks. The proportion of the chemically bound gold to metallic gold in Figure 5b, as deduced from areas under the peaks, is 7:20. Therefore, the content of chemically bound gold in the pyrite of the Xiangxi deposit reaches only 11%, *i.e.,* 50 ppm (11% of 451 ppm).
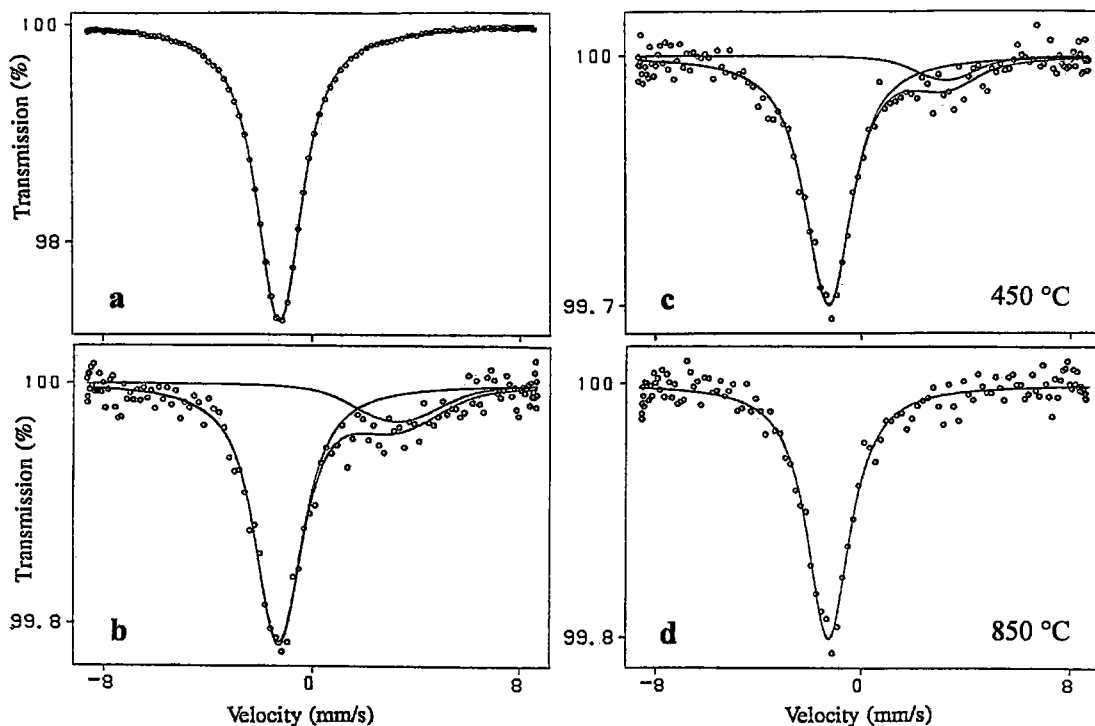
FIG. 5. [197]Au Mössbauer spectra of (a) coarse gold in a quartz vein (quartz with subordinate amounts of pyrite and chlorite), (b) metallic gold and chemical state of gold in a pyrite concentrate, (c) metallic gold and chemical state of gold in roasted pyrite concentrate (at 450°C), and (d) metallic gold in hematite, roasted from pyrite concentrate (at 850°C). All samples originate from the Xiangxi deposit.

DISCUSSION

Metallic gold

Analysis of the pyrite concentrate by [197]Au Möss-bauer spectroscopy verifies the existence of metallic gold (Au^0). Macroscopic and microscopic gold has also been observed in this study. TEM–EDS studies reveal that submicrometer-size spheres of gold (0.05–0.15 μm in diameter) precipitated on the inner growth-surfaces of pyrite and in micrometric fissures or between the grains of stibnite.

Gold on the surface of pyrite coprecipitated during the formation of the sulfides. Gold particles in micro-metric fissures or between grains of stibnite may form later than the host minerals. However, the formation of gold following sulfide precipitation, particularly stibnite crystallization (last stage of sulfide mineralization) is unlikely at Xiangxi. One possible mechanism of depo-sition of gold from ore-forming fluids may be as follows: the gold complex was adsorbed in submi-crometric fissures of sulfides just after their formation owing to its high adsorptive energy, and subsequently reduced to metallic gold, as indicated by the experiments

by Jean & Bancroft (1985), Bancroft & Hyland (1990), Mycroft et al. (1995), and Becker et al. (1997). Another possible process is the introduction of gold into the micrometric fissures in sulfides by various post-depositional processes, especially by host-mineral recrystallization and deformation, as suggested by Mumin et al. (1994). Whether gold was primarily formed by chemisorption of a gold-bearing complex at As-rich, Fe-deficient surface sites from ore fluids and by incorporation into the crystals in metastable solid-solution (Fleet et al. 1993, Fleet & Mumin 1997), or by precipitation as a solid solution in sulfides (Mumin et al. 1994) remains unknown because of limited observa-tions and data.

Constraints on the chemical state of chemically bound gold

As stated earlier, there is no satisfactory explanation for the mode of occurrence of invisible gold, particu-larly chemically bound gold in sulfides, especially in pyrite and arsenopyrite. In natural solutions, gold is commonly transported as Au^+, rather than Au^{3+}. Although Au^{3+} can also form through disproportionation

reactions from Au^+ (such as $3Au^+ = 2Au^0 + Au^{3+}$), just as Cu^{2+} does from Cu^+ (Puddephatt 1978), the content of Au^{3+} in host minerals can reach 33% at most, according to the above reaction. However, Au in arsenopyrite from Le Châtelet, France, is entirely chemically bound, amounting to 1800 ppm (Wu & Delbove 1989); similarly, Au in pyrite from the Golden Bear mine, British Columbia, occurs only as chemically bound gold; Au in another Canadian deposit, with arsenopyrite (24%) and pyrite (22%), is completely chemically bound (Friedl 1993).

Although there are some values of IS and quadrupole splitting (QS) for chemically bound gold in pyrite and arsenopyrite, the valence state of such gold cannot be determined by projecting IS and QS values on an approximate linear correlation diagram (Fig. 6). This limitation comes about because gold compounds in monovalent and trivalent states in this diagram possess a linear or two-dimensional coordination, whereas chemically bound gold in the sulfides may substitute for Fe, and therefore it would have an octahedral coordination (Bartunik *et al.* 1970). Recently, Li *et al.* (1995) concluded that chemically bound gold may occur in a negatively charged state in sulfides from a Carlin-type deposit in southern China and in hydrothermally synthesized gold-bearing pyrite and marcasite, because of the smaller binding energy, ranging from 82.5 eV to 83.5 eV for the Au $4f_{7/2}$ peak of these minerals (value of the binding energy in the state of $4f_{7/2}$ of metallic gold [Au^0]: 84.0 eV). However, in their experiments, those authors did not indicate whether the metallic gold in these sulfides is dissolved with cyanide or not; chemically bound gold in pyrite from the Carlin-type deposit can only amount to about 35% (Gao *et al.* 1992). Therefore, more investigations are required to determine whether the smaller binding energy of gold in sulfide samples relative to that of metallic gold (standard) results from the same processes that are responsible for the more negative IS values of metallic gold in our pyrite concentrates relative to standard metallic gold.

Here, we try to constrain the state of chemically bound gold in pyrite and arsenopyrite by means of crystal-chemical data and finally to determine its state in sulfides. Because there are analogies between pyrite and arsenopyrite in the characteristics of ^{197}Au Mössbauer spectroscopy, in chemical components, and in their structural coordination, we refer to experimental results of chemically bound gold in arsenopyrite in the following discussion.

Substitution of chemically bound gold for Fe^{2+} in sulfides

Arsenopyrite concentrates from Le Châtelet, France, yield a large peak originating from chemically bound gold (Wu & Delbove 1989). According to Benzaazoua (1992), gold in this deposit shows a positive correlation with arsenic and an anticorrelation with Fe in arseno-
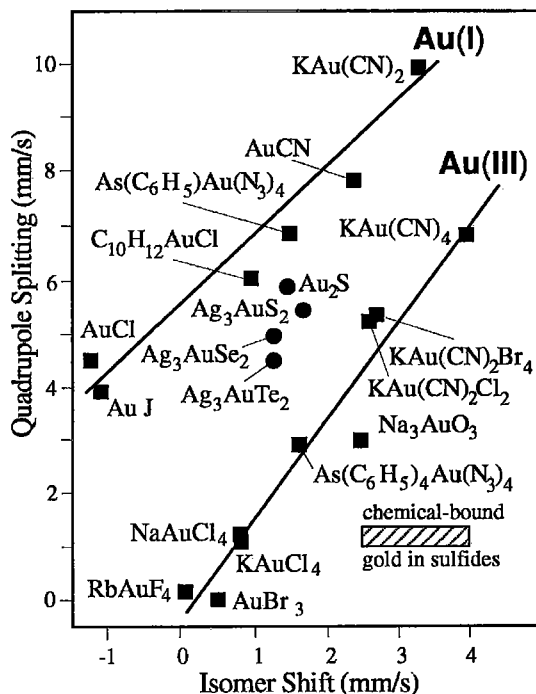

FIG. 6. Linear correlation diagram for IS (isomer shift) – QS (quadrupole splitting) of different compounds of gold (Wagner *et al.* 1994), and position of chemically bound gold (2.5 < IS < 4.0 mm/s, 1.0 < QS < 1.3 mm/s) in sulfides.

pyrite. A positive correlation coefficient between Au and As is reported by many authors (*e.g.*, Johan *et al.* 1989, Fleet *et al.* 1993, Fleet & Mumin 1997), even in the As-bearing bands of arsenopyrite (Cathelineau *et al.* 1988, Cook & Chryssoulis 1990, Arehart *et al.* 1993). An anticorrelation between Au and Fe was also reported previously (Johan *et al.* 1989; Fleet & Mumin 1997). Considering these and data of crystal chemistry, we infer that gold substitutes for Fe^{2+}, and arsenic substitutes for sulfur in pyrite and arsenopyrite.

Effects of excess arsenic in sulfides

Increasing amounts of arsenic substituting for sulfur in pyrite and arsenopyrite likely result in a lowering of the symmetry of crystal structures, that is, macroscopically, from pyrite (cubic) to arsenopyrite (orthorhombic) and to löllingite (triclinic), respectively. In terms of Mössbauer spectroscopy, the QS value of löllingite is larger than that of arsenopyrite, which again is larger than that of pyrite. This trend also implies that the substitution of As for S in arsenopyrite and löllingite results in lowering the symmetry around the Fe atom. At the same time, such a substitution increases the distance between Fe^{2+} and $[S_2]^{2-}$, $[AsS]^{2-}$ or $[As_2]^{2-}$ in pyrite,

arsenopyrite and löllingite; the distance between Fe and $[S_2]^{2-}$ and $[As_2]^{2-}$ is 2.26 Å and 2.40 Å, respectively (Vaughan & Craig 1978). Lowering the symmetry of the structure and increasing the distance between cation and anion in löllingite, arsenopyrite or in pyrite should favor a substitution of the relatively large gold ions for the smaller Fe ions.

Arsenopyrite commonly contains a higher content of chemically bound gold than pyrite, where coeval, that is, formed under identical conditions. The concentration of As in pyrite and the amount of As that exceeds the theoretical stoichiometric content of arsenic in arsenopyrite are normally much higher than that of chemically bound gold. This suggests that arsenic prefers to form $[AsAs]^{x-}$ instead of $[SAs]^{x-}$ in pyrite or in arsenopyrite; here, x is 2 for pyrite, arsenopyrite, and löllingite, because iron occurs in the 2+ state in a low-spin state in these minerals (Vaughan & Craig 1978), but for the other minerals containing Ir, Os, Ru, Pt, and Au, x is unknown. Therefore, the substitution of As for S in pyrite and arsenopyrite does not result in a disturbance of equilibrium of charge in these minerals, but results in the deformation of their crystal structures and in an increase of the distance between cations and anions.

Chemically bound gold in sulfides

A structure identical to pyrite is adopted by mineral phases such as MnS_2, CoS_2, NiS_2, RuS_2, OsS_2, $OsSb_2$, $IrSb_2$, $PtSb_2$, $PtAs_2$, and aurostibite $AuSb_2$ (Donaldson et al. 1972, Vaughan & Craig 1978). In contrast, we suggest that such octahedra also exist, in which gold occurs as the central cation; $[As_2]^{x-}$ ($AuAs_2$ most likely), $[AsS]^{x-}$ ($AuAsS$ likely), and $[S_2]^{x-}$ (AuS_2 less likely) (x as explained above) form coordination anions around gold in As-bearing pyrite or in arsenopyrite with As excess, or in löllingite, and these octahedra have a structure similar to those in pyrite (FeS_2) or, more likely, those in aurostibite ($AuSb_2$). According to [197]Au spectroscopic studies, aurostibite shows only one peak, with IS values ranging from +2.26 mm/s to +2.33 mm/s, and with a QS value of 0.00 mm/s. [121]Sb Mössbauer spectroscopy studies of this mineral yielded the same results (Friedl 1993). Therefore, the structural environment around the gold and antimony atoms in aurostibite is symmetrical, and there is only one kind of chemical and structural state for gold and antimony. However, [121]Sb Mössbauer spectroscopy studies of $OsSb_2$, $IrSb_2$, and $PtSb_2$ show that QS values in these structures decrease in the order $OsSb_2 > IrSb_2 > PtSb_2 > AuSb_2$ (Donaldson et al. 1972). In these minerals, the atomic radius increases, with Os < Ir < Pt < Au, whereas the anion $[Sb_2]^{x-}$ remains constant. In contrast, from $AuSb_2$ to the postulated octahedra of $AuAs_2$ to $AuAsS$ or AuS_2, we suggest that the octahedra of $AuAs_2$, $AuAsS$, and AuS_2 will also cause values of quadrupole splitting due to the substitution of the small anions $[S_2]^{x-}$, $[AsS]^{x-}$,

and $[As_2]^{x-}$ for the large anion $[Sb_2]^{x-}$ (x is unknown in these compounds), because $AuSb_2$ yielded a QS value of 0.00 mm/s.

IS and QS values: postulated octahedra of chemically bound gold versus sulfides

Provided the postulated octahedra of $AuAs_2$, $AuAsS$, and AuS_2 in pyrite and arsenopyrite exist, with structures and coordinations of gold similar to that of Fe in pyrite or gold in $AuSb_2$, the IS value of gold in the octahedra of $AuAs_2$, $AuAsS$, and AuS_2 will be more positive than that of gold in $AuSb_2$, because the IS value of Au is proportional to the density of the outer electrons around the gold atom, and Au in the $AuAs_2$, $AuAsS$, and AuS_2 octahedra occupies smaller spaces (namely due to the larger electron-density) than that in $AuSb_2$. Experimental results show that the IS values of chemically bound gold in pyrite and arsenopyrite (minima and maxima of +2.44 mm/s and +4.02 mm/s, respectively, with a general range of +3.0 – +4.0 mm/s) are indeed more positive than that in $AuSb_2$ (+2.26 – +2.33 mm/s) (Friedl et al. 1992, Friedl 1993).

We suggest that the structure of the postulated octahedra ($AuAs_2$, $AuAsS$, AuS_2) is transitional between that of pyrite and aurostibite. The exact structure of the octahedra determines the QS values. Friedl (1993) measured 42 samples of chemically bound gold in pyrite and arsenopyrite; 21 specimens (50% of the sample population) displayed QS values in the 1.0–1.3 mm/s range. In some sulfides, the peak for chemically bound gold can be split into two subpeaks, whereas in other sulfides it cannot, which may be due to the disappearance of structural deformations as a result of the substitution of various atoms in these minerals. The unsplit peaks are commonly wide, such as the peak of the chemically bound gold (Figs. 5b and 5c) in pyrite of the Xiangxi deposit. In addition, some peaks of chemically bound gold in pyrite and arsenopyrite are asymmetrical (Friedl 1993), with unequal line-depths, which can be explained by an anisotropic Debye–Waller factor or by a partial alignment of the crystallites in the samples. These theoretical considerations about the QS and IS values of the octahedra ($AuAs_2$, $AuAsS$, AuS_2) are in principle consistent with measured results. Therefore, the octahedra ($AuAs_2$, $AuAsS$, AuS_2) may occur locally in a chemical state in the structure of the pyrite and arsenopyrite.

Questions and suggestions

So far, we have evidence that chemically bound gold in arsenoan pyrite and in arsenopyrite most likely exists as $AuAs_2$, likely as $AuAsS$, and least likely as AuS_2, but we are unable to determine in which valence gold occurs in the octahedra in both sulfides. To solve this problem, we must consider the valence of cations in a series of minerals with a similar structure, such as FeS_2,

FeAsS, FeAs$_2$, and FeSb$_2$ (Group I), and OsSb$_2$, IrSb$_2$, PtSb$_2$, PtAs$_2$, and AuSb$_2$ (Group II). The valences of cations and anions in minerals of the first group were outlined earlier, but the valences in the second group, particularly in AuSb$_2$, are not yet clear. A single peak of aurostibite, both in ^{197}Au and ^{121}Sb Mössbauer spectroscopy, reveals that gold in this mineral occupies only one type of structural site, and occurs only in one chemical state. Although the mineral exists in nature, the valence of gold cannot be explained by the traditional valence theory. In fact, valence theory is only a model, which can explain only certain cases, but not all compounds. Although we are presently unable to explain the valence of gold in the postulated octahedra in the sulfides, this does not necessarily mean that these octahedra do not exist in nature.

We consider the energy-band theory as a feasible method to clarify the electron characteristics and configuration around the chemically bound gold, particularly in aurostibite. Solving the Schrödinger-wave equation for the mineral aurostibite will not be easy, because the mineral consists of two atoms, and anions in the mineral are paired.

CONCLUSIONS

TEM studies of sulfides reveal that submicrometer-size metallic gold occurs commonly as spheres measuring 0.07–0.15 μm in size on the surfaces of pyrite and in microfissures of stibnite. EDS data (AuLα_1 = 9.713 keV) verify that the spheres consist of gold. Studies of pyrite concentrates by ^{197}Au Mössbauer spectroscopy reveal that gold in pyrite of the Xiangxi deposit occurs mainly as metallic (89%) Au, and a subordinate fraction occurs (11%) as chemically bound Au.

We postulate that chemically bound gold occurs as octahedra, most likely of AuAs$_2$, likely of AuAsS, and less likely of AuS$_2$ in arsenopyrite or in arsenoan pyrite. The valence, structure, and coordination of the chemically bound gold in such gold-bearing octahedra are probably intermediate between those in pyrite and aurostibite.

ACKNOWLEDGEMENTS

REFERENCES

AREHART, G.B., CHRYSSOULIS, S.L. & KESLER, S.E. (1993): Gold and arsenic in iron sulfides from sediment-hosted disseminated gold deposits: implications for depositional processes. *Econ. Geol.* **88**, 171-185.

BANCROFT, G.M. & HYLAND, M.M. (1990): Spectroscopic studies of adsorption/reduction reactions of aqueous metal complexes on sulphide surfaces. *In* Mineral–Water Interface Geochemistry (M.F. Hochella, Jr. & A.F. White, eds.). *Rev. Mineral.* **23**, 511-558.

BARTUNIK, H.D., POTZEL, W., MÖSSBAUER, R.L. & KAINDL, G. (1970): Resonance spectroscopy of γ-radiation on Au(I) and Au(III) compounds. *Z. Physik* **240**, 1-16.

BECKER, U., HOCHELLA, M.F., JR. & VAUGHAN, D.J. (1997): The adsorption of gold to galena surfaces: calculation of adsorption/reduction energies, reaction mechanisms, XPS spectra, and STM images. *Geochim. Cosmochim. Acta* **61**, 3565-3585.

BENZAAZOUA, M. (1992): Caractérisation de l'or contenu dans les sulfures (pyrite et arsenopyrite) par microscopie électronique en transmission. Thèse de maîtrise, Institut National Polytechnique de Lorraine, Nancy, France.

BOYLE, R.W. (1979): The geochemistry of gold and its deposits. *Geol. Surv. Can., Bull.* **280**.

CABRI, L.J. (1988): The role of mineralogy in gold metallurgy. *CANMET, Rep.* **MSL 88-51**.

_____, CHRYSSOULIS, S.L., DE VILLIERS, J.P.R., LAFLAMME, H.H.G. & BUSECK, P.R. (1989): The nature of "invisible" gold in arsenopyrite. *Can. Mineral.* **27**, 353-362.

CATHELINEAU, M., BOIRON, M.-C., HOLLIGER, P., MARION, P. & DENIS, M. (1988): Gold in arsenopyrites: crystal chemistry, location and state, physical and chemical conditions of deposition. *Econ. Geol., Monogr.* **6**, 328-341.

CHEN XIAOQUN, GAO ANJUAN, ZHANG ZHERU & LI HEPING (1991): Studies of aurostibite. *Gold* **12**, 1-3 (in Chinese).

COOK, N.J. & CHRYSSOULIS, S.L. (1990): Concentrations of "invisible gold" in the common sulfides. *Can. Mineral.* **28**, 1-16.

DONALDSON, J.D., KJEKSHUS, A., NICHOLSON, D.G. & TRICKER, J.M. (1972): ^{121}Sb Mössbauer studies on compounds with pyrite, marcasite and arsenopyrite type structures. *Acta Chim. Scand.* **26**, 3215-3225.

FARGES, F., SHARPS, J.A. & BROWN, G.E., JR. (1993): Local environment around gold (III) in aqueous chloride solutions: an EXAFS spectroscopy study. *Geochim. Cosmochim. Acta* **57**, 1243- 1252.

1372   THE CANADIAN MINERALOGIST

FLEET, M.E., CHRYSSOULIS, S.L., MACLEAN, P.J., DAVIDSON, R. & WEISENER, C.G. (1993): Arsenian pyrite from gold deposits: Au and As distribution investigated by SIMS and EMP, and color staining and surface oxidation by XPS and LIMS. *Can. Mineral.* **31**, 1-17.

_____ & MUMIN, A.H. (1997): Gold-bearing arsenian pyrite, marcasite and arsenopyrite from Carlin Trend gold deposits and laboratory synthesis. *Am. Mineral.* **82**, 182-193.

FRIEDL, J. (1993): Untersuchungen an Goldmineralen und goldhaltigen Erzen mittels Mössbauer- Spektroskopie. Technische Universität München, Munich, Germany (with English abstr.).

_____, WAGNER, F.E., SAWICKI, J.A., HARRIS, D.C., MANDARINO, J.A. & MARION, P. (1992): ^{197}Au, ^{57}Fe and ^{121}Sb Mössbauer study of gold minerals and ores. *Hyperfine Interactions* **70**, 945-948.

GAO ZHIBIN, LI XIAOZHUANG, RONG CHUNMIAN, LI XUEBIN, WANG XIAOCHUN & SUN SHUGAO (1992): Ore-forming conditions of fine-size gold deposits, and their prediction in NW-Sichun. Unpubl. Project Report, 88 pp.

HENLEY, R. (1985): The geothermal framework of epithermal deposits. *In* Geology and Geochemistry of Epithermal Systems (B.R. Berger & P.M. Bethke, eds.). *Rev. Econ. Geol.* **2**, 1-24.

JEAN, G.E. & BANCROFT, G.M. (1985): An XPS and SEM study of gold deposition at low temperatures on sulphide mineral surfaces: concentration of gold by adsorption/reduction. *Geochim. Cosmochim. Acta* **49**, 979-987.

JOHAN, Z., MARCOUX, E. & BONNEMAISON, M. (1989): Gold-bearing arsenopyrite: mechanism of substitution of Au in the crystal structure of FeAsS. *C.R. Acad. Sci., Paris* **380**, Sér. **II**, 322-329.

JORALEMON, P. (1951): The occurrence of gold at the Getchell mine, Nevada. *Econ. Geol.* **46**, 267- 310.

LI JIULING, FENG DAMING, QI FENG & ZHANG GUILAN (1995): The existence of the negative charge state of gold in sulfide minerals and its formation mechanism. *Acta Geol. Sinica* **69**, 67-77.

MUMIN, A.H., FLEET, M.E. & CHRYSSOULIS, S.L. (1994): Gold mineralization in As-rich mesothermal gold ores of the Bogosu – Prestea mining district of the Ashanti Gold Belt, Ghana: remobilization of "invisible" gold. *Mineral. Deposita* **29**, 445-460.

MYCROFT, J.R., BANCROFT, G.M., MCINTYRE, N.S. & LORIMER, J.W. (1995): Spontaneous deposition of gold on pyrite from solutions containing Au(III) and Au (I) chlorides. I. A surface study. *Geochim. Cosmochim. Acta* **59**, 3351-3365.

NIU HUOCAI & MA DONGCHENG (1991): Fluid inclusion studies of Jiangnan-type gold deposits in western Hunan, PR China. *Acta Mineral. Sinica* **11**, 386-394 (Chinese, with English abstr.).

PUDDEPHATT, T.J. (1978): *The Chemistry of Gold.* Elsevier, Amsterdam, The Netherlands.

STILLWELL, F.L. & EDWARDS, A.B. (1946): An occurrence of sub-microscopic gold in the Dolphim East Lode, Fiji. *Austral. Inst. Mining Metall.* **141**, 31-46.

VAUGHAN, D.J. & CRAIG, J.R. (1978): *Mineral Chemistry of Metal Sulfides.* Cambridge University Press, London, U.K.

WAGNER, F.E., MARION, P. & REGNARD, J.-R. (1986): Mössbauer study of the chemical state of gold in gold ores. *In* Gold 100, Proc. Int. Conf. on Gold. **2**. Extractive Metallurgy of Gold. South African Institute of Mining and Metallurgy, Johannesburg, South Africa.

_____, _____ & _____ (1988): ^{197}Au Mössbauer study of gold ores, mattes, roasted products, and gold minerals. *Hyperfine Interactions* **41**, 851-854.

_____, SAWICKI, J.A., FRIEDL, J., MANDARINO, J.A., HARRIS, D.C. & CABRI, L.J. (1994): ^{197}Au Mössbauer study of the gold-silver ditellurides sylvanite, krennerite and calaverite. *Can. Mineral.* **32**, 189-201.

_____, SWASH, P.M. & MARION, P. (1989): A ^{197}Au- and ^{57}Fe-Mössbauer study of the roasting of refractory gold ores. *Hyperfine Interactions* **46**, 681-688.

WU XIN & DELBOVE, F. (1989): Hydrothermal synthesis of gold-bearing arsenopyrite. *Econ. Geol.* **84**, 2029-2032.

YANG SIXUE (1995): Die Xiangxi Au–Sb–W Lagerstätte in NW Hunan/China – Geochemie und Metallogenese. Dissertation, Freie Universität Berlin, Berlin, Germany (with English abstr.).

ZHANG ZHERU, WANG QINGDUO, LIAO FENGXIAN & LI HEPING (1991): The studies on manner of occurrence of submicrometric gold in arenopyrite. *J. Guilin College of Geol.* **11**, 150-153 (Chinese, with English abstr.).